Electric-Alignment Immobilization of Liquid Crystalline Colloidal Nanosheets with the Aid of a Natural Organic Polymer

doi: https://doi.org/10.1021/acs.langmuir.9b00651

Electric-Alignment Immobilization of Liquid Crystalline Colloidal Nanosheets with the Aid of a Natural Organic Polymer

Emiko Mouri[1,2], Akari Irie[1], Teruyuki Nakato[1,2,*]

[1] Department of Applied Chemistry, Kyushu Institute of Technology

1-1 Sensui-cho, Tobata, Kitakyushu, Fukuoka 804-8550, Japan.

[2] Strategic Research Unit for Innovative Multiscale Materials, Kyushu Institute of Technology, 1-1 Sensui-cho, Tobata, Kitakyushu, Fukuoka 804-8550, Japan.

Keywords: Inorganic nanosheets, Colloidal liquid crystal, Niobate, Agar, Electric alignment, Sol–gel transition

Abstract

Inorganic nanosheets obtained by exfoliation of layered crystal in water form colloidal liquid crystals, and their alignment can be controlled by an electric field. In order to realize the immobilization of the electrically aligned niobate nanosheets without external forces, an aqueous gelator, agar, is introduced to the niobate nanosheet system to utilize the thermosensitive sol–gel transition property of agar. Alignment of nanosheets in a niobate–agar system is performed by applying an electric field above the sol–gel transition temperature and then the sample is cooled down followed by cooling below the transition temperature with the electric field turned off.

The aligned structure is kept for more than 24 h after removal of the electric field. The concentration of agar is a key parameter for both the orientation of nanosheets and the retention of the orientation.

Introduction

Macroscopically structured assemblies of colloidal particles prepared by their controlled organization is important for developing novel advanced materials, in which the structure in macroscopic size at a scale larger than sub-millimeters directly reflects the macroscopic properties of materials.

Macroscopic properties are much more important than microscopic properties in practical usage [1]. Colloidal particles are more practical than molecules as building blocks for constructing macroscopically structured assemblies because their particle size ranges in the order of nanometers to submicrons. Macroscopically structured assemblies have been realized by using colloidal crystals [2], Pickering emulsions [3], and colloidsomes [4]. In a general sense, spherical particles are utilized for constructing organized systems because of their wide variety of choices and high monodispersity. However, anisotropic particles such as 2D plates and 1D rods are promising candidates for more complex assembly formation because their shape anisotropy have an advantage over spherical particles in the fabrication of anisotropic assemblies [5–7].

Among the anisotropic particles, inorganic nanosheets prepared from layered crystals through exfoliation possess high aspect ratio due to their thickness of around 1 nm and lateral length of several tens of nanometers to micrometers [8, 9]. In addition, they have robust structures due to inorganic crystallinity; these help maintain greater stability the of 2D morphology compared with organic materials. The high aspect ratio of inorganic nanosheets is known to induce stable liquid crystalline phases [10-13]. In the past two decades, nanosheet liquid crystals (LCs) have been discovered, and various

macroscopically structured assemblies have been organized from nanosheet LCs [14–16]. In these assemblies, nanosheet orientations have been controlled at macroscopic scales by external forces such as electric and magnetic fields, shared forces, and laser radiation pressures [17-29]. The obtained macroscopic structures open up various applications of nanosheets, such as meta-materials and photonic crystals.

Macroscopic structures organized under external forces usually collapse if the applied force is removed. Although polymerization of organic monomers added to nanosheet LCs under external forces can immobilize the nanosheet orientation, covalent cross-linking between the monomer units prohibits further orientational change of nanosheets, which restricts the application of nanosheet LCs with structural switching induced by external forces [15, 30]. Reversible immobilization of nanosheet LCs is required to retain the reversibility of nanosheet orientation by external forces.

One of the general strategies of reversibly immobilizing colloidal particles in solvents is the employment of a sol–gel transition phenomenon with physical or chemical interactions [31–33]. The solutions and colloids of certain organic molecules and polymers reversibly undergo physical sol–gel transition with external stimuli such as temperature and pH change [34–36]. Coexisting colloidal particles that are movable in a sol state are reversibly immobilized in a gel state induced by the sol–gel transition

of the colloid. By applying this process to nanosheet LCs, we can immobilize nanosheet orientation achieved under external forces and reversibly relax the immobilized orientation. Nanosheets aligned in a sol state can be reversibly immobilized by the sol–gel transition of the colloidal LC.

In the present study, we have examined the immobilization of an electrically aligned colloidal LC of niobate nanosheets obtained by exfoliation of layered hexaniobate crystallites in water. We have already shown that liquid crystalline hexaniobate nanosheets align under an electric field as liquid crystalline molecules usually do [23]. Furthermore, we have constructed macroscopic hierarchical structures reflecting the 2D nature of inorganic nanosheets [14, 37, 38] with the combined strategy of LC domain growth and nanosheet alignment under external electric fields. We have also found that the macroscopic structure can be tuned by several parameters such as nanosheet concentration, applied voltage, and cell thickness to produce a wide variety of macroscopic structures.

However, in the above-mentioned electric manipulation, nanosheet alignment is no longer retained when the electric field is removed. It is inconvenient to keep supplying electricity for maintaining the structure in applications for standalone devices and remote-controlling systems. Thus, the retention of the electrically induced

structures is an important task for manipulating niobate nanosheet LCs.

An aqueous gelator is necessary for realizing the immobilization of the electrically aligned niobate nanosheets by sol–gel transition because niobate nanosheet LCs are aqueous colloids. We choose agar, a natural biocompatible polymer, for this purpose. It undergoes temperature-induced sol–gel transition; agar gels at room temperature turn to sols at around 40 °C [39–42]. Hence, we use sol–gel transition to create electric alignment and subsequent immobilization of nanosheets with the strategy schematically shown in Figure 1. We have combined the temperature change of the aqueous nanosheet colloid included in agar with electric alignment.

Experimental Section

Sample Preparation

Niobate nanosheet colloids were prepared by the exfoliation of layered niobate $K_4Nb_6O_{17}$ using the same procedure described in a previous paper [37, 38, 43]. The average niobate nanosheet size used here was 2.1 μm. Agar powder (Kanto Chemical Co. Inc., Tokyo, Japan) was dissolved in pure water and heated up to 90 °C. Solutions with different agar concentrations were prepared. A niobate–agar colloid was prepared by adding a certain amount of niobate sample to agar solution at 50 °C and stirred for

5 min. The agar concentration in the mixture ranged from 0.1 to 1.0 wt%. The concentration of niobate nanosheets was set to 5 g L^{-1}, at which the niobate colloid was biphasic, i.e., a mixture of isotropic and liquid crystalline phases [43–45].

Observation for Sol–Gel Transition

An agar, or niobate–agar colloid sample in a glass vial (8 mm in diameter) was heated to 50 °C on a hot plate and then cooled to room temperature. The sol–gel status of the sample at each temperature was judged by visual observation after the sample vial was turned upside down. In order to confirm the critical minimum agar concentration for achieving gelation, we examined the sol–gel transition at varied agar concentrations.

Electric Application

A niobate–agar sol sample was subjected to electric application for the nanosheet orientation. The colloid sample was injected into a thin-layer ITO cell with a cell gap of 100 μm, and was kept at 50 °C by placing on a thermally controlled plate [29]. The cell was left at this temperature on the controlling plate for 1 min to relax the sample flow in the cell. An AC electric voltage of 2–5 V at 50 kHz was then applied for 8 min at 50 °C to induce the nanosheet orientation at the sol state. The

direction of electric application is normal to the cell surface. The electric and heat applications were stopped simultaneously, and then the cell was cooled to room temperature with the electric field off to induce gelation or viscous nature. In this cooling process, the sol–gel transition, or more exactly transition from fluid sol to viscous sol in the samples subjected to the electric alignment experiments as described later, occurred upon decrease of the temperature to the sol–gel transition point at around 30–40 °C. Although temperature increase by the applied electric field was possible, its influence on the viscosity change of the colloids was negligible in our experiments. The nanosheet alignment induced by the electric application was expected to be confined in the gel or viscous sol. We observed the temporal structural change up to 24 h after the electric application under a BX-51 optical microscope (Olympus, Tokyo, Japan) with crossed polarizers.

Results and Discussion

Appropriate Agar Concentration for Sol–Gel Transition and Electric Response of the Niobate–Agar Colloids

We first determined the appropriate agar concentration of the niobate–agar colloid, as well as the concentration that allows electric manipulation of niobate

nanosheets and their immobilization. Agar solutions cause the sol–gel transition at 30–40 °C [39–42]. Figure 2 shows photographs of agar solutions and niobate–agar colloids at 40 °C and 25 °C with various agar concentrations (0.1–0.8 wt%) at a fixed niobate concentration (5 g L^{-1}). The photographs at 25 °C were taken both 15 s and 1 min after the vial was turned upside down to qualitatively evaluate the viscosity. When the agar concentration was 0.1 wt%, both the agar solution and the niobate–agar colloid did not show sol–gel transition upon temperature reduction from 40 °C to 25 °C, as evidenced by the fluid nature of the samples shown in Figure 2. At an agar concentration of 0.2 wt%, the sol samples did not completely convert to gels but their viscosities increased upon cooling of the samples to 25 °C, as qualitatively shown by the photographs of the temporal states. At an agar concentration of 0.8 wt%, a temperature-induced sol–gel transition was clearly observed for sols at 40 °C and gels at 25 °C. Similar behavior of the agar and niobate–agar samples suggests the absence of apparent agar–niobate interactions that change the sol–gel transition drastically. However, there is a small difference in gel stiffness. Gel containing niobate is somewhat softer than the agar gel itself suggesting by the gel meniscus in inclined flask (Fig. S1). This difference would suggest the presence of weak interactions between niobate nanosheets and agar at a molecular level. Because agarose, which is the main

constituent of agar, has many hydroxy groups, and niobate nanosheets are anionic, electrostatic repulsions can work between niobate nanosheets and agar molecules. This means that niobate nanosheets do not work as cross-linking points in the gelation of agar. Thus, niobate nanosheets would prevent the direct interactions between agarose molecules by niobate-agarose interaction to weaken the gel stiffness, but this effect is very minor in sol-gel transition of our samples.

We examined the electric response of liquid crystalline niobate nanosheets in sol-state agar at concentrations of 0, 0.2, 0.4, and 0.8 wt% at 50 °C. Preliminary, we also confirmed that the agar/niobate system that can be manipulated by electric application at 50 ºC cannot be electrically manipulated at room temperature. Figure 3 shows POM (Polarized Optical Microscope) images of niobate–agar colloids and an agar solution before and after the application of the AC electric field (5 V, 50 kHz). For samples without agar, i.e., a simple niobate nanosheet colloid, the POM image was dark, indicating niobate nanosheets lying in parallel to the substrate, but the image after the electric application for 8 min was bright because of birefringence (Figure 3a). This change is in accordance with our previous results [38]. It indicates alignment of niobate nanosheets parallel to the electric field, i.e., perpendicular to the substrate as already discussed in our previous paper [23].

Electrically induced nanosheet alignment was also observed in the niobate–agar colloid with 0.2 wt% agar concentration in the sol state (50 °C), as evidenced by the appearance of birefringence after the AC voltage application (Figure 3c). Agar molecules are not the origin of the birefringence because they are dissolved isotropically in water and thus non-birefringent images before and after the electric field application (Figure 3b). In contrast, the niobate–agar colloids with agar concentration above 0.4 wt% did not much respond to the electric field (Figures 3d and e): limited fraction of niobate nanoheets respond to the electric field based on the some spots with birefringence in Figure 3d and e, which is due to the higher viscosity of the samples. A higher concentration of ager induces higher viscosity of samples even in the sol state, which makes it difficult to electrically manipulate niobate nanosheets.

On the basis of these results, we determined that the appropriate agar concentration in the niobate–agar colloids with 5 g L^{-1} niobate nanosheets is 0.2 wt% for realizing electric alignment with immobilization of the aligned structure. Although the niobate–agar colloid does not gel completely at this agar concentration, its viscosity increases with cooling of the sample from 40 °C to 25 °C, as mentioned above (Figure 2). This viscosity increase with the temperature change is large enough to retain the electric alignment of niobate nanosheets (vide infra).

Immobilization of the Electrically Aligned Niobate Nanosheets in the Niobate–Agar Colloid

We examined the retention of the electric alignment of niobate nanosheets through temperature-induced gelation of the colloid by agar. The niobate–agar colloid (5 g L^{-1} niobate, agar) was first heated to 50 °C to ensure the sol state, and the AC voltage was applied for 8 min to cause the electric nanosheet alignment (vide supra). The sample was cooled down to 25 °C to convert from sol to gel, and then the AC voltage application was terminated. For comparison, a niobate colloid (5 g L^{-1}) without agar was also treated in the same sequence.

Alteration of the electrically aligned nanosheets with this process is indicated by POM images shown in also Figure 3. The POM image of the niobate colloid sample without agar 10 min after the termination of the AC voltage application indicates reduction of the birefringent area relative to that of the sample upon application of the electric field (Figures 3a, AC 8min and 10 min after AC off). This indicates that the electrically aligned nanosheets have started the relaxation of alignment after the removal of the electric field. After 24 h, the alignment was completely lost, as evidenced by the dark POM image (Figure 3a, 24 h after AC off). However, the

niobate–agar colloid produced birefringent POM images 24 h after AC voltage removal (Figure 3c, 24 h after AC off). The birefringent area is almost the same as that under the electric field. These results demonstrate retention of the electric alignment of niobate nanosheets in the niobate–agar colloid for more than 24 h when the colloid temperature was reduced after the electric nanosheet alignment. The concentration of agar is a key parameter for both the orientation of nanosheets and the retention of the orientation, as summarized in Figure 4.

Effect of AC Voltage

We investigated the effect of the applied AC voltage on the electric nanosheet alignment and its retention in the niobate–agar colloid. Figure 5 shows the temporal changes in POM images a niobate–agar sample subjected to a sequence of electric fields in the sol state and its removal in the gel state with applied voltages of 2 to 5 V. The samples subjected to AC voltage higher than 3 V show both strong birefringence under the electric field and its retention after the removal of the electric field. The samples subjected to electric fields lower than 2.75 V show only weak birefringence under the electric field and a large decrease after the AC voltage cutoff.

These results indicate that the niobate–agar colloid effectively retains the electric alignment of niobate nanosheets only when the nanosheet alignment is attained. The lower degree of electric alignment at an applied voltage of less than 2.75 V is ascribed to the presence of agar; the niobate colloid without agar responds to the 2 V electric field, similarly to 5 V. The introduction of agar to niobate nanosheet colloid increases the viscosity of the colloid even at the sol state. Hence, low AC voltages are insufficient to turn the nanosheet direction. In contrast, fast relaxation of the insufficiently aligned nanosheets at the viscous sol state (observed at Figure 5, 2.75 V and 2V) is related to the cooperative effect of nanosheets originating from their liquid crystallinity. The clear difference between the images obtained at 3 V and 2.75 V in Figure 5 suggests that majority alignment of the nanosheets has an effect on the retention of nanosheet alignment. AC voltage of 2.75V insufficiently aligns some nanosheets but most nanosheets are not aligned with lying parallel to the cell surface. In this case, cooperative effects between the aligned nanosheets, i.e., minor components and non-aligned nanosheets, i.e., dominant components would assist relaxation of the alignment. Our recent study on optical manipulation of niobate nanosheets revealed that cooperation between the liquid crystalline nanosheets expands their alignment to nanosheets that are not directly manipulated by the external force [29].

Textural Difference in the Electrically Aligned Nanosheets

However, the texture formed by the electric application in the niobate–agar mixture is somewhat different from that formed in niobate colloids, as suggested by Figure 5. The single niobate colloid shows a texture characterized by small birefringent domains of aligned nanosheets spreading over the entire area. In contrast, the niobate–agar colloids show a mosaic-like location of the birefringent area segregated from dark regions. This indicates segregation of the domains of electrically aligned niobate nanosheets from the non-birefringent agar domains.

We assumed that this is caused by the difference in the dispersion status of niobate nanosheets in the colloid, which is partly explained by the change in viscosity due to the addition of agar. Increasing the viscosity by addition of agar delays the settling of niobate nanosheets in the cell, and the niobate dispersion status in the cell therefore is different from the one without agar. Because colloidal particles generally suffer from thermal perturbation during their sedimentation [46], delayed settling of the particles can change their distribution. Hence, it is reasonable to ascribe the difference in nanosheet distribution with and without agar to the difference in the settling rate.

The other possible explanation for segregation is phase separation in the niobate–agar binary system due to the depletion effect [47, 48]. In general, a

multi-component colloidal system without any specific interaction between the colloidal particles tends to show phase separation due to the depletion effect. This can be the case for binary colloids of niobate nanosheets and agar molecules.

Conclusions

In summary, electrically aligned colloidal inorganic nanosheets prepared by exfoliation of layered hexaniobate can be immobilized by introducing a natural gelator, agar, to the colloid. The immobilization is realized by a temperature-driven viscosity change related to the sol–gel transition of agar. The immobilization of nanosheet orientation is realized at an appropriate agar concentration, which determines the colloid viscosity and allows the nanosheet alignment by an electric field at high temperature, as well as the immobilization of alignment at low temperature. The nanosheet orientation is retained 24 h after the electric application at an agar concentration of 0.2 wt%, although the macroscopic structure of niobate nanosheets with agar induced by electric application is somewhat different from those one without agar. The compatibility of the orientation control and its retention is possible only at certain limited agar concentrations. This immobilization of liquid colloidal nanosheet alignment is a step

forward for creating smart materials in which the structure inside the medium can be controlled reversibly in a less energy-consuming way.

Acknowledgments

This work was partly supported by JSPS KAKENHI (no. 16K14095 for T. N. and no. 18K04729 for E. M.).

Reference

1. Therien-Aubin, H.; Lukach, A.; Pitch, N.; Kumacheva, E., Coassembly of nanorods and nanospheres in suspensions and in stratified films. *Angew. Chem., Int. Ed.* **2015,** *54*, 5618-5622.

2. Yamanaka, J.; Suzuki, Y.; Nozawa, J.; Sawada, T., In-situ observation of colloidal crystallization. *Prog. Cryst. Growth Charact. Mater.* **2016,** *62*, 413-416.

3. Binks, B. P., Colloidal particles at a range of fluid-fluid interfaces. *Langmuir* **2017,** *33*, 6947-6963.

4. Dinsmore, A. D.; Hsu, M. F.; Nikolaides, M. G.; Marquez, M.; Bausch, A. R.; Weitz, D. A., Colloidosomes: Selectively permeable capsules composedof colloidal particles. *Science* **2002**, *298*, 1006-1009.

5. Zhang, J.; Lang, P. R.; Meyer, M.; Dhont, J. K., Synthesis and self-assembly of squarelike PbCrO4 nanoplatelets via micelle-mediated depletion attraction. *Langmuir* **2013,** *29*, 4679-4687.

6. Sharma, P.; Ward, A.; Gibaud, T.; Hagan, M. F.; Dogic, Z., Hierarchical organization of chiral rafts in colloidal membranes. *Nature* **2014,** *513*, 77-80.

7. Shopsowitz, K. E.; Qi, H.; Hamad, W. Y.; Maclachlan, M. J., Free-standing mesoporous silica films with tunable chiral nematic structures. *Nature* **2010,** *468*, 422-425.

8. Ma, R. Sasaki, T., Nanosheets of oxides and hydroxides: Ultimate 2D charge-bearing functional crystallites. *Adv. Mater.* **2010,** *22*, 5082-5104.

9. Nakato, T. Kawamata, J., Takagi S., Inorganic Nanosheets and Nanosheet-based Materials; Springer; 1st ed. 2017.

10. Onsager, L., The effects of shape on the interaction of colloidal particles. *Ann. N. Y. Acad. Sci.* **1949,** *51*, 627-659 .

11. Gabriel, J. C. P.; Davidson, P., Mineral liquid crystals from self-assembly of anisotropic nanosystems. In *Colloid Chemistry I*, Antonietti, M., Ed. Springer Berlin Heidelberg: Berlin, Heidelberg, 2003; 119-172.

12. Sonin, A. S., Inorganic lyotropic liquid crystals. *J. Mater. Chem.* **1998,** *8*, 2557–2574.

13. Lekkerkerker, H. N.; Vroege, G. J., Liquid crystal phase transitions in suspensions of mineral colloids: new life from old roots. *Philos Trans A Math Phys Eng Sci* **2013,** *371*, 20120263.

14. Nakato, T.; Nono, Y.; Mouri, E.; Nakata, M., Panoscopic organization of anisotropic colloidal structures from photofunctional inorganic nanosheet liquid crystals. *Phys. Chem. Chem. Phy.* **2014,** *16*, 955-962.

15. Inadomi, T.; Ikeda, S.; Okumura, Y.; Kikuchi, H.; Miyamoto, N., Photo-induced anomalous deformation of poly(*N*-isopropylacrylamide) gel hybridized with an inorganic nanosheet liquid crystal aligned by electric field. *Macromol. Rapid. Commun.* **2014**, *35*, 1741-1746.

16. Geng, F.; Ma, R.; Nakamura, A.; Akatsuka, K.; Ebina, Y.; Yamauchi, Y.; Miyamoto, N.; Tateyama, Y.; Sasaki, T., Unusually stable ~100-fold reversible and instantaneous swelling of inorganic layered materials. *Nat. Commun.* **2013,** *4*, 1632-1639.

17. J.-C.P. Gabriel, F. C., B.J. Lemaire, H. Desvaux, P. Davidson, P. Batail, Swollen liquid-crystalline lameller phase based on extended solid-like sheets. *Nature* **2001,** *413*, 504-508.

18. Zhang, S.; Kumar, S., Carbon nanotubes as liquid crystals. *Small* **2008,** *4*, 1270-1283.

19. Paineau, E.; Antonova, K.; Baravian, C.; Bihannic, I.; Davidson, P.; Dozov, I.; Impēror-Clerc, M.; Levitz, P.; Madsen, A.; Meneau F.; Michot, L. J., Liquid-crystalline nematic phase in aqueous suspensions of a disk-shaped natural beidellite clay. *J. Phys. Chem. B* **2009,** *113*, 15858–15869.

20. Nakato, T.; Miyamoto, N., Liquid Crystalline Behavior and Related Properties of Colloidal Systems of Inorganic Oxide Nanosheets. *Materials* **2009,** *2*, 1734-1761.

21. Dozov, I.; Paineau, E.; Davidson, P.; Antonova, K.; Baravian, C.; Bihannic, I.; Michot, L. J., Electric-field-induced perfect anti-nematic order in isotropic aqueous suspensions of a natural beidellite clay. *J. Phys. Chem. B* **2011,** *115*, 7751-7765.

22. Kim, J. E.; Han, T. H.; Lee, S. H.; Kim, J. Y.; Ahn, C. W.; Yun, J. M.; Kim, S. O., Graphene oxide liquid crystals. *Angew. Chem. Int. Ed.* **2011,** *50*, 3043-3047.

23. Nakato, T.; Nakamura, K.; Shimada, Y.; Shido, Y.; Houryu, T.; Iimura, Y.; Miyata, H., Electrooptic response of colloidal liquid crystals of inorganic oxide nanosheets prepared by exfoliation of a layered niobate. *J. Phys. Chem. C* **2011,** *115*, 8934-8939.

24. Miyamoto, N.; Nakato, T., Liquid crystalline inorganic nanosheet colloids derived from layered materials. *Isr. J. Chem.* **2012,** *52*, 881-894.

25. Hong, S.-H.; Shen, T.-Z.; Song, J.-K., Electro-optical characteristics of aqueous graphene oxide

dispersion depending on ion concentration. *J. Phys. Chem. C* **2014,** *118*, 26304-26312.

26. L.L. Wu, M. O., M. Takata, A. Saeki, S. Seki, Y. Ishida, T. Aida, Magnetically induced anisotropic orientation of graphene oxide locked by in situ hydrogelation *ACS Nano* **2014,** *8*, 4640-4649.

27. Shen, T. Z.; Hong, S. H.; Song, J. K., Electro-optical switching of graphene oxide liquid crystals with an extremely large Kerr coefficient. *Nat. Mater.* **2014,** *13*, 394-399.

28. Narayan, R.; Kim, J. E.; Kim, J. Y.; Lee, K. E.; Kim, S. O., Graphene oxide liquid crystals: discovery, evolution and applications. *Adv. Mater.* **2016,** *28*, 3045-3068.

29. Tominaga, M.; Nagashita, T.; Kumamoto, T.; Higashi, Y.; Iwai, T.; Nakato, T.; Suzuki, Y.; Kawamata, J., Radiation pressure induced hierarchical structure of liquid crystalline inorganic nanosheets. *ACS Photonics* **2018,** *5*, 1288-1293.

30. Kim, Y. S.; Liu, M.; Ishida, Y.; Ebina, Y.; Osada, M.; Sasaki, T.; Hikima, T.; Takata, M.; Aida, T., Thermoresponsive actuation enabled by permittivity switching in an electrostatically anisotropic hydrogel. *Nat. Mater.* **2015,** *14*, 1002-1007.

31. Niu, J.; Wang, D.; Qin, H.; Xiong, X.; Tan, P.; Li, Y.; Liu, R.; Lu, X.; Wu, J.; Zhang, T.; Ni, W.; Jin, J., Novel polymer-free iridescent lamellar hydrogel for two-dimensional confined growth of ultrathin gold membranes. *Nat. Commun.* **2014,** *5*, 3313.

32. Takeoka, Y.; Watanabe, M., Template synthesis and optical properties of chameleonic poly(*N*-isopropylacrylamide) gels using closest-packed self-assembled colloidal silica crystals *Adv. Mater.* **2003,** *15*, 199-201.

33. Holtz, J. H.; Asher, S. A., Polymerized colloidal crystal hydrogel films as intelligent chemical sensing materials. *Nature* **1997,** *389*, 829–832.

34. Yanagisawa, Y.; Nan, Y.; Okuro, K.; Aida, T. Mechanically robust, readily repairable polymers via tailored noncovalent cross-linking. *Science* **2018,** *359*, 72-76.

35. Chen, Q.; Zhu, L.; Zhao, C.; Wang, Q.; Zheng, J., A robust, one-pot synthesis of highly mechanical and recoverable double network hydrogels using thermoreversible sol-gel polysaccharide. *Adv. Mater.* **2013,** *25*, 4171-4176.

36. Dong, S.; Luo, Y.; Yan, X.; Zheng, B.; Ding, X.; Yu, Y.; Ma, Z.; Zhao, Q.; Huang, F., A dual-responsive supramolecular polymer gel formed by crown ether based molecular recognition. *Angew. Chem. Int. Ed.* **2011,** *50*, 1905-1909.

37. Nono, Y.; Mouri, E.; Nakata, M.; Nakato, T., Flow-induced assembly of colloidal liquid crystalline nanosheets toward unidirectional macroscopic structures. *J. Nanosci. Nanotechnol.* **2016,** *16*, 2967-2974.

38. Nakato, T.; Nono, Y.; Mouri, E., Textural diversity of hierarchical macroscopic structures of colloidal liquid crystalline nanosheets organized under electric fields. *Colloid Surf A Physicochem Eng Asp* **2017,** *522*, 373-381.

39. Arnott, S.; Fulmer, A.; Scott, W. E.; Dea, I. C. M.; Moorhouse, R.; Rees, D. A., The agarose

double helix and its function in agarose gel structure. *J. Mol. Biol.* **1974,** *90*, 269-284.

40. Mohammed, Z. H.; Hember, M. W. N.; Richardson, R. K.; Morris, E. R. Kinetic and equilibrium processes in the formation and melting of agarose gels. *Carbohydr. Polym.* **1998,** *36*, 15-26.

41. Zhou, J.; Zhou, M.; Caruso, R. A. Agarose template for the fabrication of macroporous metal oxide structures. *Langmuir* **2006,** *22*, 3332-3336.

42. Pinto, M. N.; Martinez-Gonzalez, J.; Chakraborty, I.; Mascharak, P. K., Incorporation of a theranostic "two-tone" luminescent silver complex into biocompatible agar hydrogel composite for the eradication of ESKAPE pathogens in a skin and soft tissue infection model. *Inorg. Chem.* **2018,** *57*, 6692-6701.

43. Miyamoto, N.; Nakato, T., Liquid crystalline nature of $K_4Nb_6O_{17}$ nanosheet sols and their macroscopic alignment. *Adv. Mater.* **2002,** *14*, 1267-1270.

44. Nakato, T.; Miyamoto, N.; Harada, A., Stable liquid crystalline phases of colloidally dispersed exfoliated layered niobates. *Chem. Commun.* **2004,** 78-79.

45. Nakato, T.; Miyamoto, N., Liquid crystalline nanosheet colloids with controlled particle size obtained by exfoliating single crystal of layered niobate $K_4Nb_6O_{17}$. *J. Phys. Chem. B* **2004,** *108*, 6152-6159.

46. Everett, D. H., Basic Principles of Colloid Science; The Royal Society of Chemistry; 1988.

47. Asakura, S.; Oosawa, F. On Interaction between two bodies immersed in a solution of macromolecules. *J. Chem. Phys.* **1954,** *22*, 1255.

48. Ilett, S. M.; Orrock, A.; Poon, W. C. K.; Pusey, P. N., Phase behavior of a model colloid-polymer mixture. *Phys. Rev. E* **1995,** *51*, 1344-1352.

TOC

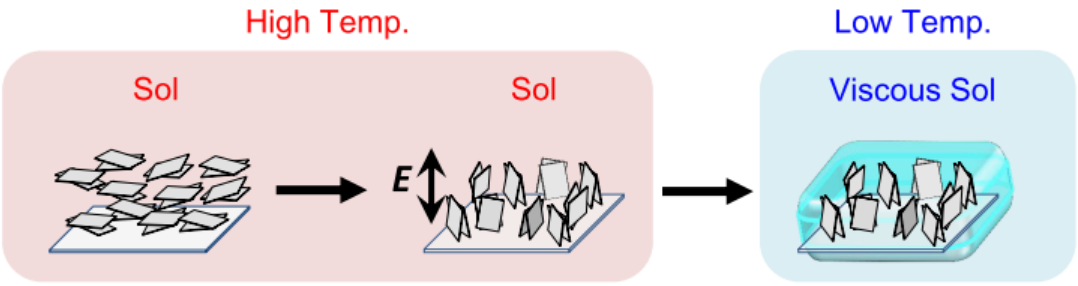

Immobilization of Electrically-induced Alignment of Nanosheets